Closing the loop for hydrogen storage: Facile regeneration of $NaBH_4$ from its hydrolytic product

Yongyang Zhu, [a] Liuzhang Ouyang, *[ab] Hao Zhong, [a] Jiangwen Liu, [a] Hui Wang, [a] Huaiyu Shao, *[,c] Zhenguo Huang*[,d], and Min Zhu[a]

a: School of Materials Science and Engineering, Guangdong Provincial Key Laboratory of Advanced Energy Storage Materials, South China University of Technology, Guangzhou, 510641, People's Republic of China.

b: China-Australia Joint Laboratory for Energy & Environmental Materials, Key Laboratory of Fuel Cell Technology of Guangdong Province, Guangzhou, 510641, People's Republic of China.

c: Joint Key Laboratory of the Ministry of Education, Institute of Applied Physics and Materials Engineering (IAPME), Department of Physics and Chemistry, Faculty of Science and Technology, University of Macau, Macau SAR, China. Email: hshao@um.edu.mo

d: School of Civil and Environmental Engineering, University of Technology Sydney, Sydney, NSW, 2007, Australia. Email: zhenguo.huang@uts.edu.au

* Author to whom correspondence should be addressed.

Liuzhang Ouyang, E-mail address: meouyang@scut.edu.cn Tel: 86-20-87114253, Fax: 86-20-87114253, Huaiyu Shao (hshao@um.edu.mo), and Zhenguo Huang (zhenguo.huang@uts.edu.au)

Abstract:

Sodium borohydride ($NaBH_4$) is among the most studied hydrogen storage materials since it is able to deliver high purity H_2 at room temperature with controllable kinetics via hydrolysis, but its regeneration from the hydrolytic product has been challenging. Herein we report a facile method to regenerate $NaBH_4$ with high yield and low costs. The hydrolytic product $NaBO_2$ in aqueous solution reacts with CO_2 forming $Na_2B_4O_7{\cdot}10H_2O$ and $NaCO_3$, both of which are ball milled with Mg under ambient conditions to form $NaBH_4$ with a high yield close to 80 %. Compared with previous studies, this new approach avoids expensive reducing agent such as MgH_2, bypasses the energy-intensive dehydration procedure to remove water from $Na_2B_4O_7{\cdot}10H_2O$, and does not requires high-pressure H_2 gas, therefore leading to much reduced costs. This method is expected to effectively close the loop of $NaBH_4$ regeneration and hydrolysis, enabling a wide deployment of $NaBH_4$ for hydrogen storage.

Keywards: borohydride, regeneration, hydrolysis, hydrogen storage

Graphical Abstract:

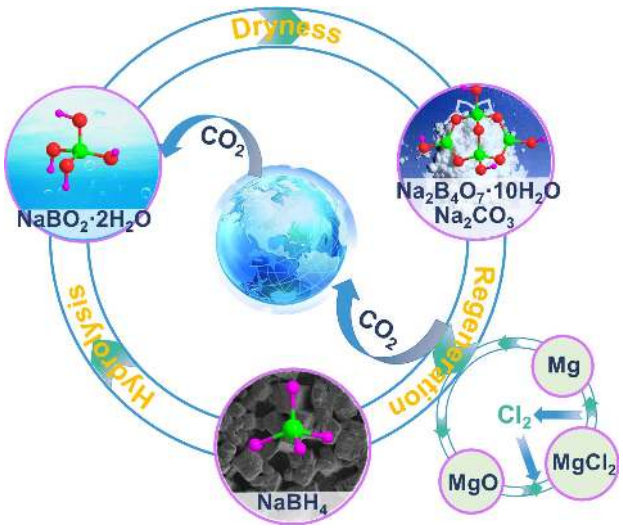

1 Introduction

Hydrogen has been deemed as an ideal energy carrier due to its high energy density by weight, high abundance, and environmental friendliness [1-3]. However, wide utilization of hydrogen energy has been hampered by a few barriers with one of them associated with storage. Due to its low energy density by volume, hydrogen has been conventionally compressed or liquefied to improve the density. However, these physical processes cause large energy penalty and special care is always required when operating under high pressure or cryogenic conditions. Materials-based hydrogen storage has therefore received strong attention since it has attractive features such as higher capacity, better safety, and milder operation conditions.

Sodium borohydride ($NaBH_4$) is among the most studied candidates as a hydrogen storage material. $NaBH_4$ can release hydrogen via hydrolysis with good controllability, high hydrogen purity, high gravimetric hydrogen storage capacity and environmentally benign by-products [4-6]. The hydrolysis of $NaBH_4$ is typically expressed by the following reaction:

$$NaBH_4 + (2+x)H_2O \rightarrow NaBO_2 \cdot xH_2O + 4H_2 \quad (1)$$

The spent fuel is normally hydrated sodium metaborate ($NaBO_2$) in aqueous solution [7]. The regeneration of $NaBH_4$ from the hydrolytic product so far has featured high costs and low yields.

$NaBO_2$ in aqueous solution reacts with CO_2 in air forming $Na_2B_4O_7 \cdot 10H_2O$ and $NaCO_3$ according to the following reaction:

$$4NaBO_2 \cdot xH_2O + CO_2 + (10-4x)\ H_2O \rightarrow Na_2B_4O_7 \cdot 10H_2O + Na_2CO_3 \quad (2)$$

$Na_2B_4O_7 \cdot 10H_2O$ is the main constituent of naturally abundant borax mineral. It is therefore highly appealing to develop a simple, efficient and affordable approach to generate $NaBH_4$ from $Na_2B_4O_7 \cdot 10H_2O$.

Currently, two types of raw materials, H_2 (H°) and metal hydride (H^-) have been used as hydrogen sources in the (re)generation of $NaBH_4$. For example, $NaBH_4$ can be synthesized by annealing $Na_2B_4O_7$ with Na and SiO_2 under high pressure H_2 (over 3 MPa) at elevated temperature (400–500°C) [8]. This method is of high cost because the reaction conditions are harsh and a considerable amount of sodium metal is needed. Recently, the preparation of $NaBH_4$ has been carried out by annealing the dehydrated borax ($Na_2B_4O_7$) with low-cost magnesium (Mg) at a high temperature (550°C) and high H_2 pressure (2.5MPa) [9]. However, this process is also energy intensive and dangerous. The process can be further optimized by ball milling $Na_2B_4O_7$ with magnesium hydrides (MgH_2) with a maximum yield of 78% [10, 11]. The use of expensive MgH_2, however, makes mass production by this method less feasible. It should also note that high energy is required to obtain $Na_2B_4O_7$ by dehydrating $Na_2B_4O_7 \cdot 10H_2O$ at approximately 600°C [12].

Herein, we present a new method where H^+ in the coordinate water in $Na_2B_4O_7$ can be directly used as a hydrogen source to prepare $NaBH_4$. In the new procedure, a mixture of $Na_2B_4O_7 \cdot xH_2O$ (x=5, 10) and Na_2CO_3 is obtained by exposing $NaBO_2$ aqueous solution to CO_2 and then drying at a temperature of < 54 °C. Ball milling the mixture with Mg at room temperature and atmospheric pressure leads to the formation of $NaBH_4$ with a high yield of 78.9%. Compared with the literature procedures that

require dehydrated $Na_2B_4O_7$, MgH_2, high pressure H_2, and/or high temperatures, the new method utilize low cost materials and operate under mild reaction conditions, which allow for facile scaled up manufacturing.

2 Experimental

2.1 Materials

Sodium tetraborate decahydrate ($Na_2B_4O_7 \cdot 10H_2O$) and sodium tetraborate pentahydrate ($Na_2B_4O_7 \cdot 5H_2O$) powders were purchased from Aladdin (Shanghai, China, ACS-grade) and Xiya Reagent (Shandong, China, 99% purity), respectively. Magnesium powder (Mg, 99.8% purity), sodium borohydride ($NaBH_4$, ≥98%) and ethylenediamine ($C_2H_8N_2$, ≥99% purity) were obtained from Sigma-Aldrich and stored and handled in a glove box (MIKROUNA, China) filled with argon with O_2 and H_2O concentrations below 0.1 ppm. Sulfuric acid (H_2SO_4 (GR)), sodium carbonate (Na_2CO_3, 99.5% purity), sodium hydroxide (NaOH, ≥99%), potassium iodate (KIO_3, AR-grade), potassium iodide (KI, ≥99%), starch indicator (≥99%), and sodium thiosulfate ($Na_2S_2O_3$, AR-grade) were purchased from Aladdin. All reagents were used as received without further purification. DI water (18.25 MΩ resistance) obtained from a water purification system (Unique-S10, Guangzhou, China) was used to prepare aqueous solution.

2.2 Synthesis of $NaBH_4$

Mechano-chemical synthesis of $NaBH_4$ was carried out by ball milling $Na_2B_4O_7 \cdot xH_2O$ (x=5, 10), Na_2CO_3 and Mg in a shaker mill (QM-3C, Nanjing, China) at 1000 or 1200 cycle per min (CPM) under ambient temperature. For each experiment,

in a glove box filled with Ar, 1 g of reactants with a specific molar ratio was loaded in a 80 mL jar with a ball-to-powder weight ratio of 50:1. Two different sized steel balls were used. To prevent overheating, the milling process was performed by alternating 30 min of milling with 30 min of rest. $NaBH_4$ was extracted from the reaction products using anhydrous ethylenediamine under Ar atmosphere at room temperature. Ethylenediamine was added to the ball-milled product in a closed flask which was stirred by a magnetic stirrer. Polytetrafluoroethylene membrane (0.25 μm in pore size) was used to separate the solution from solids. The filtrate was dried in a freeze dryer (Martin Christ, Alpha 1-2LD plus, Germany) to obtain $NaBH_4$, whose quantity was determined using iodimetric analysis [13]. The yield of $NaBH_4$ was calculated according to the following equation [14]:

$$\text{Yield } (NaBH_4) = \frac{obtained\ mass\ NaBH4}{theoretical\ mass\ NaBH4} \times 100\%$$

The theoretical amount was based on a full conversion meaning that 1 mole $Na_2B_4O_7 \cdot xH_2O$ (x=5, 10) is converted to 4 mole of $NaBH_4$.

2.3 Hydrolysis of $NaBH_4$

Hydrolysis of $NaBH_4$ was carried out using an apparatus (Fig. S1 in Supporting Information) described in one previous study [15]. About 0.05 g $NaBH_4$, synthesized or commercial, was hydrolysed in 1.0 mL aqueous solution with 2 wt% $CoCl_2$ at room temperature. $NaBH_4$ was first added into a glass tube and $CoCl_2$ aqueous solution was then injected into the glass tube. The hydrogen evolution was monitored via registering the weight of discharged water using an electronic scale connected to a computer.

2.4 Characterization

The phase composition of the solid powders was investigated by a wide-angle X-ray diffractometer (XRD). The X-ray diffraction patterns were recorded at ambient temperature using a Rigaku MiniFlex 300/600 in the range from 10 to 90° diffraction angle with CuKα radiation (λ = 0.15418 nm) at operating parameters of 40 mA and 45 kV. The samples were smeared on a glass slide in a home-made device and then covered with Scotch tape to prevent exposure to air. Fourier transform infrared spectroscopy (FTIR) was performed on a Nicolet IS50 spectrometer in the region of 4000-400 cm^{-1}. Solid-state ^{11}B magic angle spinning nuclear magnetic resonance (MAS NMR) (Bruker-AVANCE III HD 400) and solution-state (D_2O+0.5M NaOD) NMR (Bruker-AVANCE III HD 500) spectra were collected. The morphology of the samples was inspected by a scanning electron microscope (SEM) (Zeiss, Supra-40) and also a transmission electron microscope (TEM) (Jeol, JEM-2100). Identities of the gaseous products formed during ball milling were determined by a mass spectrometer (MS, Hiden-Qic 20).

3 Results and discussion

3.1 Regeneration and hydrolysis cycle

One key challenge in utilizing $NaBH_4$ for hydrogen storage lies in its regeneration. Herein we developed a facile procedure to regenerate $NaBH_4$ from its CO_2 treated hydrolytic product (Fig. 1a). $NaBH_4$ can be successfully synthesized by ball milling a mixture of Mg, $Na_2B_4O_7{\cdot}10H_2O$, and Na_2CO_3 at ambient condition. Fig. 1b shows the XRD qualitative analysis of the powders after 20h milling of a mixture of Mg, $Na_2B_4O_7{\cdot}10H_2O$, and Na_2CO_3 in a mole ratio of 24.75:1:1. The diffraction peaks are

indexed to $NaBH_4$ and MgO.

$NaBH_4$ was isolated from the as-milled product, and its identity and morphology were studied using XRD, FT-IR, NMR, SEM, and TEM. XRD pattern of commercial $NaBH_4$ (Fig. 1c(2)) show ten peaks at 25.1°, 28.9°, 41.4°, 49.0°, 51.3°, 60.0°, 66.0°, 68.0°, 75.5°, and 81.0°, corresponding to (111), (200), (220), (311), (222), (400), (331), (420), (422), and (511) of $NaBH_4$ (ICDD 00-009-0386), respectively. The synthesized $NaBH_4$ displays the same XRD pattern as the commercial $NaBH_4$ (Fig. 1c(3)). The FT-IR bands (2200-2400 and 1125 cm^{-1}, corresponding to the B-H stretching and deformation of pure $NaBH_4$, respectively [16-18]) of the isolated $NaBH_4$ are in good agreement with the those of commercial $NaBH_4$ (Fig. S2a). The XRD and FT-IR results are also consistent with the previous studies on $NaBH_4$ synthesis [18-21]. The BH_4^- anion is further confirmed by NMR analysis (Fig.S2b) [22]. Similar to commercial $NaBH_4$, the synthesized $NaBH_4$ exists in cubic particles with sizes of several microns (Fig. S3). Selected area electron diffraction (SAED) pattern also indicates the success in obtaining crystalline $NaBH_4$ (Fig. 1d and Fig. S4).

According to the results obtained from various techniques (XRD, FTIR, NMR, SEM, and TEM), we can conclude that high quality $NaBH_4$ with crystallography and microstructure similar to commercial $NaBH_4$ was successfully synthesized by directly ball milling $Na_2B_4O_7 \cdot 10H_2O$ and Na_2CO_3 with Mg in Ar at room temperature. The synthesis conditions are very mild compared with the previous studies in which $NaBH_4$ was produced via $NaBO_2$ reacting with Mg at 350°C under 7 MPa H_2 [23] or $Na_2B_4O_7$ reacting with Mg at 550°C under 2.5 MPa H_2 [9].

For a closed-loop application, hydrogen evolution performance of the regenerated $NaBH_4$ is particularly important. Fig. 1e shows the hydrogen production curves of prepared $NaBH_4$. The prepared $NaBH_4$ showed good hydrolysis properties and produced 2317 mL/g hydrogen totally in 1.8 min. After the hydrolytic aqueous solution was naturally dried up in air, solid $Na_2B_4O_7 \cdot 10H_2O$ (ICDD ref. 01-075-1078) powers were obtained, as evidenced by XRD patterns (Fig. 1f) and FT-IR spectra (Fig. S5). Another set of characteristic diffraction peaks can be indexed to $Na_3H(CO_3)_2 \cdot 2H_2O$ which is composed of Na_2CO_3 and $NaHCO_3$. The transformation of Na_2CO_3 into $NaHCO_3$ occurs in the following reaction:

$$Na_2CO_3\ (aq) + CO_2 + H_2O \rightarrow 2NaHCO_3 \quad (3)$$

$NaHCO_3$ can be avoided by regulating the exposure of the hydrolytic aqueous solution to air. This is supported by experiments that only $Na_2B_4O_7 \cdot 10H_2O$ and Na_2CO_3 can be obtained by tuning the exposure of $NaBO_2$ aqueous solution to CO_2 (Fig. S6).

We propose a pathway to close the cycle of $NaBH_4$ hydrolysis and regeneration (Fig. 1a). Comparing with the literature methods, current procedure features low-cost starting materials, mild reactions at room temperature, and requiring no high pressure H_2. The energy efficiency of regeneration can be estimated by systematic modeling, which is beyond the scope of the current work. One important step in the complete cycle is the reformation of Mg metal. Although electrochemical process of extracting Mg is energy intensive, it is widely adopted industrially. Overall, this represents a promising cycle pathway for large-scale application of $NaBH_4$ as a hydrogen carrier.

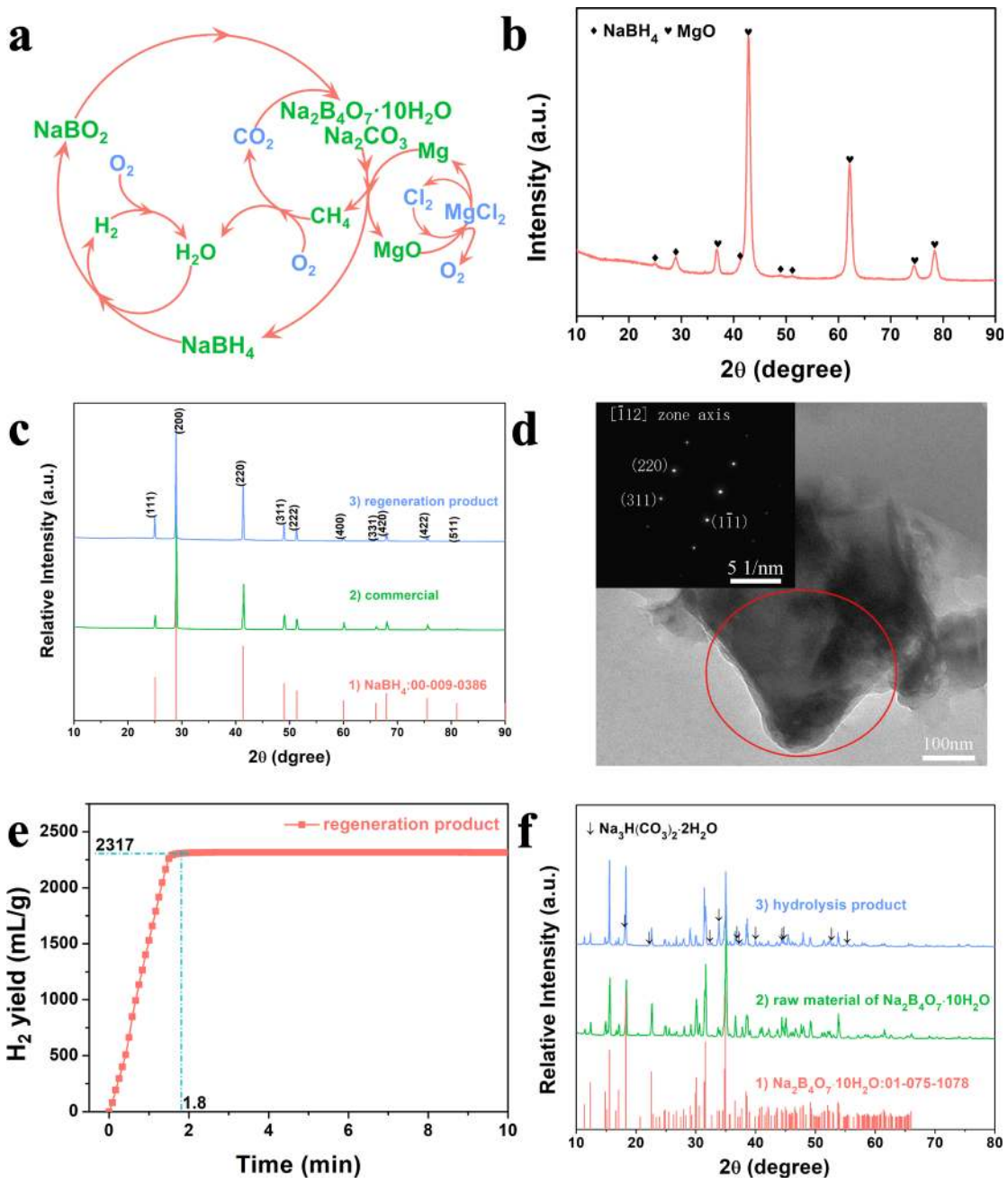

Fig. 1 (a) A closed system of $NaBH_4$ hydrolysis and regeneration. (b) XRD pattern of products obtained via ball milling a mixture of Mg, $Na_2B_4O_7 \cdot 10H_2O$, and Na_2CO_3 in 24.75:1:1 molar ratio for 20 h at 1000 CPM. (c) XRD patterns of 1) standard PDF card of $NaBH_4$, 2) commercial and 3) synthesized $NaBH_4$. (d) TEM image and SAED pattern of synthesized $NaBH_4$. (e) Hydrolysis curve of the prepared $NaBH_4$ in 2 wt% $CoCl_2$ aqueous solution. (f) XRD patterns of 1) standard PDF card of $Na_2B_4O_7 \cdot 10H_2O$, 2) raw $Na_2B_4O_7 \cdot 10H_2O$, and 3) compounds obtained after hydrolytic aqueous

solution naturally dried up in air.

3.2 Reaction mechanism

To understand the reaction, $Na_2B_4O_7 \cdot 10H_2O$, Na_2CO_3, and Mg mixtures were ball milled for relatively short periods. The XRD diffraction peaks of $Na_2B_4O_7 \cdot 10H_2O$ become invisible after 5 min milling, along with the appearance of diffraction peaks of $Na_2B_4O_7 \cdot 5H_2O$ (Fig. 2a), in agreement with FT-IR results (Fig. 2b(2) and Fig. S7). The actual formula of $Na_2B_4O_7 \cdot 5H_2O$ and $Na_2B_4O_7 \cdot 10H_2O$ are $Na_2B_4O_5(OH)_4 \cdot 3H_2O$ and $Na_2B_4O_5(OH)_4 \cdot 8H_2O$, respectively, according to the chemical structures [24]. Hydrogen can be detected in this period from the MS of the gas atmosphere (Fig. S8). After 10 min of ball milling, the intensity of diffraction peaks of $Na_2B_4O_7 \cdot 5H_2O$ decreases significantly. As the milling increases to 30 min, XRD diffraction peaks of MgO become highly visible while those of $Na_2B_4O_7 \cdot 5H_2O$ and Na_2CO_3 almost disappear. Although the diffraction peaks of $NaBH_4$ are invisible, the B-H group can be detected by FT-IR (Fig. 2b(4)). The absorption bands of BO_3^{3-} (1500-1300 cm^{-1}) and BO_4^{5-} (1150-950 cm^{-1}) originally present in $[B_4O_5(OH)_4]^{2-}$, and of CO_3^{2-} (1450-1400 cm^{-1}, 877 cm^{-1}) originally present in Na_2CO_3 become very weak and then vanish completely from the spectra (Fig. 2b). As the milling time reaches 5 h, the (200) diffraction peak of $NaBH_4$ appears.

Considering the observation of $Na_2B_4O_7 \cdot 5H_2O$ and H_2 after 5 min, the first step of the reaction is assumed as follows:

$$Na_2B_4O_7{\cdot}10H_2O \rightarrow Na_2B_4O_7{\cdot}5H_2O + 5H_2O \quad (4)$$

$$2H_2O + Mg \rightarrow Mg(OH)_2 + H_2 \quad (5)$$

Under the experiment conditions, the following reactions will subsequently occur [25, 26]:

$$Mg + Mg(OH)_2 \rightarrow 2MgO + H_2 \quad (6)$$

$$H_2 + Mg \rightarrow MgH_2 \quad (7)$$

With increasing milling time, $NaBH_4$, MgO, and also CH_4 (Fig. S8 and Fig. S9) were observed which is associated with this reaction:

$$Na_2B_4O_7{\cdot}5H_2O + Na_2CO_3 + 15MgH_2 \rightarrow 4NaBH_4 + 20MgO + CH_4 + 10H_2 \quad (8)$$

The overall reaction equation is therefore can be expressed in the following equation:

$$Na_2B_4O_7{\cdot}10H_2O + Na_2CO_3 + 20Mg \rightarrow 4NaBH_4 + 20MgO + CH_4 \quad (9)$$

This reaction is calculated to be favourable in thermodynamics (ΔG^{o}_{298k}= -1326.18 kJ/mol of $NaBH_4$).

In this closed-loop regeneration (Fig. 1a), CH_4 can be collected and converted to CO_2, which is then used to produce Na_2CO_3. Mg can be regenerated via the commercial method, where MgO is first converted to $MgCl_2$ and Mg is obtained by electrolysis of $MgCl_2$.

MgH_2 was not observed in this study, probably because it was consumed *in-situ* due to its high activity. This is in agreement with a previous study where MgH_2 was proposed as an intermediate during $NaBH_4$ regeneration via ball milling $NaB(OH)_4$ and Mg [17]. The formation of methane is likely due to the reaction between Na_2CO_3 and

MgH_2 [27, 28]. H_2 was not in the overall reaction (eqn 9) but was observed by MS, which is due to the nature of gas-solid reaction between H_2 and Mg, where it is hard to achieve 100 % conversion.

To further elucidate the reaction mechanism, the ball milled products were characterized by solid-state ^{11}B magic-angle spinning (MAS) NMR (Fig. 2c). After 10 min of ball milling, only $[B_4O_5(OH)_4]^{2-}$ is detected (Fig. 2c(2)). The resonance observed at $\approx$-13.4 ppm in Fig. 2c(3) after 30 min milling demonstrates the formation of intermediate H_2BOH [21, 29]. The reaction transformation of $[B_4O_5(OH)_4]^{2-}$ is therefore proposed as shown in Fig. 2d. The unit of $[B_4O_5(OH)_4]^{2-}$ contains two BO_4 tetrahedra and two BO_3 triangles as showed in Fig. 2d(1). The B-O bond (average bond length: 1.3683 Å) in BO_3 triangles is stronger than the one (average bond length: 1.4418 Å) in BO_4 tetrahedra [30]. Thus, the B-O in BO_4 tetrahedra preferentially breaks, and B forms bond with the H in MgH_2 and the O forms bond with Mg. It is reasonable to assume that three intermediates are formed (Fig. 2d(2-4)). Thermodynamically, Mg is more likely to bond with oxygen to form a more stable compound, MgO (ΔG_f^o of MgO: -569.3 kJ/mol oxygen; ΔG_f^o of B_2O_3: -398.1 kJ/mol oxygen) [31]. Therefore, B-O and Mg-H in the B-O-Mg-H intermediate break and the B-H and MgO are formed (Fig. 2d(2,4)). The breaking of the (B)-O-H (O bonded with sp^2 boron) in Fig. 2d(5) results into formation of intermediate "H_2BOH", which is detected in NMR spectra (Fig. 2c(3)). According to the literature [21], B in "H_2BOH" is Lewis acidic and could accept H^- from MgH_2. As a result, "BH_4^-" and MgO are generated. In addition, the "OH^-" that is bonded with sp^3 boron (Fig. 2d(3,4)), is substituted by H^- in MgH_2 forming "BH_4^-",

which agrees with previous studies [17].

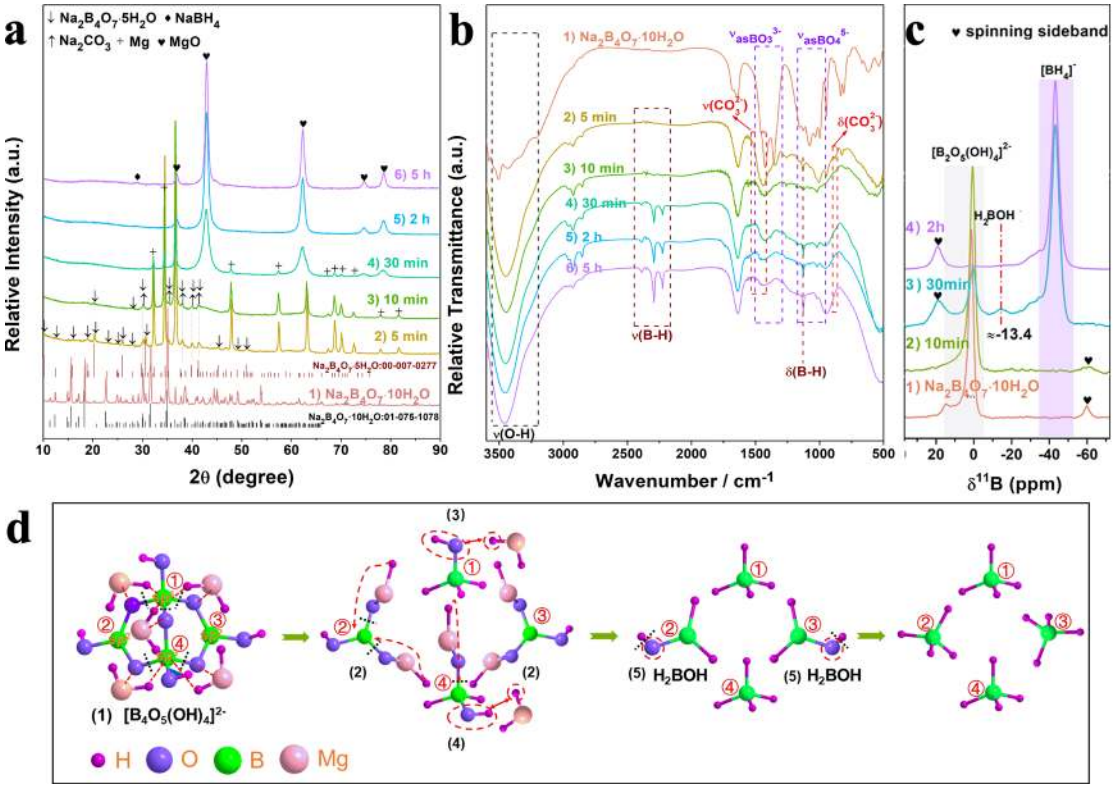

Fig. 2. (a) XRD patterns and (b) FT-IR spectra of 1) raw $Na_2B_4O_7 \cdot 10H_2O$; products obtained after ball milling Mg, $Na_2B_4O_7 \cdot 10H_2O$, and Na_2CO_3 mixtures (in 18:1:1 molar ratio) at 1200 CPM for different durations 2) 5 min, 3) 10 min, 4) 30 min, 5) 2 h and 6) 5 h. (c) Solid-state ^{11}B NMR spectra of 1) raw $Na_2B_4O_7 \cdot 10H_2O$; products obtained after ball milling for different durations 2) 10 min, 3) 30 min, 4) 2 h. (d) Proposed reaction mechanism between Mg, Na_2CO_3, and $Na_2B_4O_7 \cdot 10H_2O$ to form $NaBH_4$.

3.3 Yield of $NaBH_4$

Efforts have been made to optimize the yield of $NaBH_4$ by ball milling CO_2 treated hydrolytic products (a mixture of $Na_2B_4O_7 \cdot 10H_2O$ and Na_2CO_3) with Mg. Fig. 3a shows the XRD patterns of the products obtained by ball milling Mg, $Na_2B_4O_7 \cdot 10H_2O$, and Na_2CO_3 in a 18:1:1 molar ratio for different durations. After 2.5 h of ball milling,

the diffraction peaks of raw materials disappear, along with the appearance of strong diffraction peaks of MgO. Although the diffraction peaks of $NaBH_4$ are invisible, the typical BH_4 bands (2200-2400 and 1125 cm^{-1}) are detectable by FT-IR (Fig. 3b(1)), which indicates the formation of $NaBH_4$ after 2.5h ball milling. As milling time increases to 10h, the diffraction peaks assigned to Fe_2B become visible (Fig. 3a(3)). With further increase in milling time, the diffraction peaks of Fe_2B become stronger while the characteristic FT-IR bands of $NaBH_4$ become weaker. The FT-IR results indicate that the yield of $NaBH_4$ firstly increases and then decreases with the milling time (Fig. 3b). Iodometric analysis was carried to quantify $NaBH_4$ after its isolation from the ball-milled product. The relationship between the yield and milling time is consistent with FT-IR results (Fig. 3b, c), reflecting the fact that $NaBH_4$ is decomposed after long-time ball-milling. This is likely due to the reaction between $NaBH_4$ and Fe (peeling off the balls and jar after long-time ball-milling), as evidenced by the formation of more Fe_2B as milling time increases (Fig. 3a). The highest yield among the five durations for the mixture with 18:1:1 molar ratio is about 17.4% after 5 h of ball milling (Fig. 3c).

The impact of Mg loading on the yield was also studied (Fig. 3d). For 20h milling, the yield increased when more Mg was used, and it was ~46.9% for a molar ratio of 20.25:1:1 (Mg: $Na_2B_4O_7 \cdot 10H_2O$: Na_2CO_3), and reached the maximum of 75.7% for a ratio of 24.75:1:1. The highest yield of 78.9% was obtained after 30 h of ball milling for the sample with 24.75:1:1 mole ratio (Fig. 3c). For this particular batch, the yield after 5 h (38.0%) is already much higher than that with 18:1:1, and the XRD diffraction

peaks of $NaBH_4$ are clearly visible (Fig. 3f). Yields can be improved by increasing the amount of Mg used, which is consistent with previous studies [10, 11, 14, 19, 31, 32]. With a high loading of Mg, powders do not stick to the jar and balls, resulting in better the ball-milling efficiency. In addition, more Mg leads to better contact among all the reactants resulting in favorable yield. Limited by the ball mill machine, only two milling speeds, 1000 and 1200 CPM, were tried, which proves that ball mill speed, ie energy, does impact the yield. Although the energy is higher at 1200 CPM, we fail to obtain better yields under any circumstances, especially for a low molar ratio (Fig. 3d). This is because more Fe peels off the balls and jar for small amount of Mg at high speed and promotes $NaBH_4$ decomposition (Fig. 3e).

We have also found that when $Na_2B_4O_7{\cdot}10H_2O$ and $Na_2B_4O_7{\cdot}5H_2O$ were ball milled simultaneously with Na_2CO_3 and Mg in a molar ratio of 0.6:0.4:1:22, $NaBH_4$ was also successfully synthesized (Fig. S10). Mg can also be replaced by Al or Ca to synthesize $NaBH_4$ (Fig. S11). More research is needed to optimize the yields of $NaBH_4$ from these reactions.

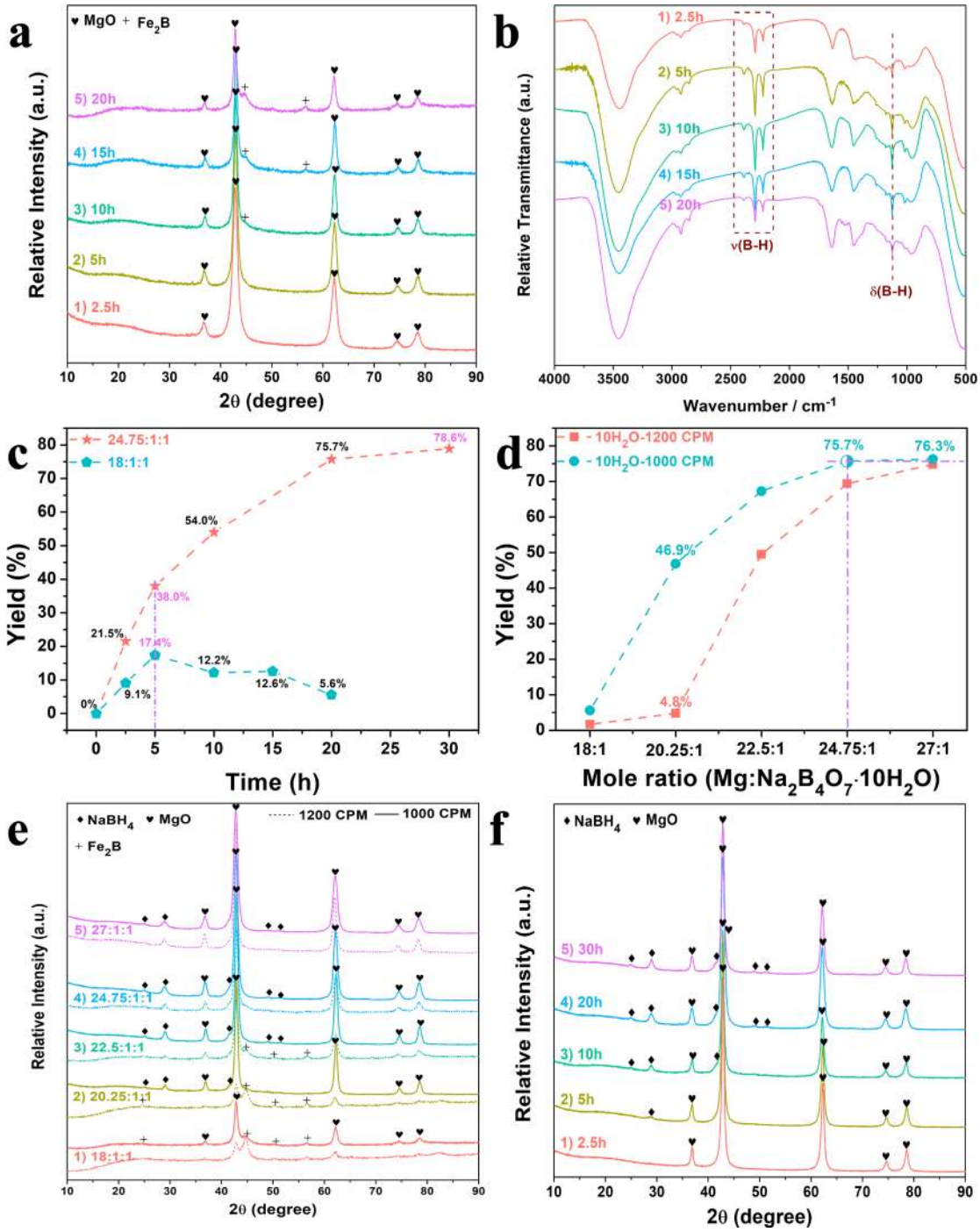

Fig. 3. (a) XRD patterns and (b) FT-IR spectra of the products obtained after ball milling Mg, $Na_2B_4O_7·10H_2O$, and Na_2CO_3 mixtures (in 18:1:1 molar ratio) at 1000 CPM for different durations. (c) Yields of $NaBH_4$ with reactants in different molar ratios at 1000 CPM for different durations. (d) Yields of $NaBH_4$ and (e) XRD patterns of the products obtained after ball milling Mg and $Na_2B_4O_7·10H_2O$ in different molar ratios ($Na_2B_4O_7·10H_2O$ and Na_2CO_3 were fixed at 1:1 molar

ratio) for 20h at 1000 CPM and 1200 CPM, respectively. (f) XRD patterns of the products obtained via ball milling Mg, $Na_2B_4O_7·10H_2O$, and Na_2CO_3 in a molar ratio of 24.75:1:1 at 1000 CPM for different durations.

4. Conclusions

In summary, we present a closed pathway for utilizing $NaBH_4$ for hydrogen storage. The regeneration of $NaBH_4$ can be achieved by ball milling its CO_2 treated hydrolytic product ($Na_2B_4O_7·10H_2O$ and Na_2CO_3) and Mg under ambient condition, with the yield being among the highest reported so far. This process outperforms the literature methods in several key aspects. First of all, the current yield is the best among the reported literatures [10, 14, 19, 33-35] (Table S1). Secondly, the direct use of $Na_2B_4O_7·10H_2O$ avoids high temperatures (over 600°C [12]) required to dehydrate $Na_2B_4O_7·10H_2O$. Thirdly, this process does not need expensive MgH_2, which is usually obtained by high-temperature reaction between Mg and H_2. When comparing this method with reported process using MgH_2, Na_2CO_3 and $Na_2B_4O_7$ [10], the cost of the raw materials in this method is reduced by 24-fold (Table S2). This indicates a promising pathway for large-scale application of $NaBH_4$ as a hydrogen carrier.

Acknowledgement

This work was financially supported by the National Key R&D Program of China (No. 2018YFB15-02100), Foundation for Innovative Research Groups of the National Natural Science Foundation of China (No. NSFC51621001), National Natural Science

Foundation of China Projects (Nos. 51771075) and by the Project Supported by Natural Science Foundation of Guangdong Province of China (2016A030312011). Author Ouyang also thanks Guangdong Province Universities and Colleges Pearl River Scholar Funded Scheme (2014). Z.H. acknowledges support under the Australian Research Council's Discovery Projects funding scheme (project number DP170101773). Shao acknowledges support from Macau Science and Technology Development Fund (FDCT) (Project No.: 0062/2018/A2 and 118/2016/A3).

References

[1] A.F. Dalebrook, W. Gan, M. Grasemann, S. Moret, G. Laurenczy, Chem. Commun., 49 (2013) 8735-8751.
[2] I.P. Jain, Int. J. Hydrogen Energy, 34 (2009) 7368-7378.
[3] L. Schlapbach, A. Züttel, Nature, 414 (2001) 353-358.
[4] Y. Kojima, Y. Kawai, H. Nakanishi, S. Matsumoto, J. Power Sources, 135 (2004) 36-41.
[5] R.B. Biniwale, S. Rayalu, S. Devotta, M. Ichikawa, Int. J. Hydrogen Energy, 33 (2008) 360-365.
[6] E.Y. Marreroalfonso, A.M. Beaird, T.A. Davis, M.A. Matthews, Ind. Eng. Chem. Res., 48 (2009) 3703-3712.
[7] M.A. Budroni, S. Garroni, G.R.C. Mulas, M. Rustici, J. Phys. Chem. C, 121 (2017) 4891-4898.
[8] F. Schubert, K. Lang, W. Schlabacher, in, DE Pat. 1067005, 1959.
[9] İ. Kayacan, Ö.M. Doğan, B.Z. Uysal, Int. J. Hydrogen Energy, 36 (2011) 7410-7415.
[10] Z.P. Li, N. Morigazaki, B.H. Liu, S. Suda, J. Alloys Compd., 349 (2003) 232-236.
[11] C. Çakanyıldırım, M Gürü, Energy Sources, 34 (2012) 1104-1113.
[12] A. Ekmekyapar, A. Ahmet Baysar, A. Künkül, Ind. Eng. Chem. Res., 36 (1997) 3487-3490.
[13] D.A. Lyttle, E.H. Jensen, W.A. Struck, Anal. Chem., (1952) 1843-1844.
[14] L. Kong, X. Cui, H. Jin, J. Wu, H. Du, T. Xiong, Energy Fuels, 23 (2009) 5049-5054.
[15] L. Ouyang, M. Ma, M. Huang, R. Duan, H. Wang, L. Sun, M. Zhu, Energies, 8 (2015) 4237-4252.
[16] L.Z. Ouyang, H. Zhong, Z.M. Li, Z.J. Cao, H. Wang, J.W. Liu, X.K. Zhu, M. Zhu, J. Power Sources, 269 (2014) 768-772.
[17] L. Ouyang, W. Chen, J. Liu, M. Felderhoff, H. Wang, M. Zhu, Adv. Energy Mater., 7 (2017) 1700299.

[18] H. Zhong, L.Z. Ouyang, J.S. Ye, J.W. Liu, H. Wang, X.D. Yao, M. Zhu, Energy Storage Materials, 7 (2017) 222-228.
[19] C.L. Hsueh, C.H. Liu, B.H. Chen, C.Y. Chen, Y.C. Kuo, K.J. Hwang, J.R. Ku, Int. J. Hydrogen Energy, 34 (2009) 1717-1725.
[20] M. Huang, H. Zhong, L. Ouyang, C. Peng, X. Zhu, W. Zhu, F. Fang, M. Zhu, M. Huang, H. Zhong, J. Alloys Compd., 729 (2017) 1079-1085.
[21] C. Lang, Y. Jia, J. Liu, H. Wang, L. Ouyang, M. Zhu, X. Yao, Int. J. Hydrogen Energy, 42 (2017) 13127-13135.
[22] J. Huang, Y. Yan, A. Remhof, Y. Zhang, D. Rentsch, Y.S. Au, P.E.D. Jongh, F. Cuevas, L. Ouyang, M. Zhu, Dalton Trans., 45 (2016) 3687-3690.
[23] J.F. Hull, Y. Himeda, W.H. Wang, B. Hashiguchi, R. Periana, D.J. Szalda, J.T. Muckerman, E. Fujita, Nat. Chem., 4 (2012) 383-388.
[24] I. Waclawska, J. Therm. Anal., 43 (1995) 261-269.
[25] Y. Chen, J.S. Williams, J. Alloys Compd., 217 (1995) 181-184.
[26] I.P. Jain, C. Lal, A. Jain, Int. J. Hydrogen Energy, 35 (2010) 5133-5144.
[27] E. Mukhina, A. Kolesnikov, V. Kutcherov, Scientific reports, 7 (2017) 5749.
[28] J.Y. Chen, L.J. Jin, J.P. Dong, H.F. Zheng, G.Y. Liu, Chin. Chem. Lett., 19 (2008) 475-478.
[29] A.C. Stowe, W.J. Shaw, J.C. Linehan, B. Schmid, T. Autrey, Phys. Chem. Chem. Phys., 9 (2007) 1831-1836.
[30] Y. Wang, S. Pan, X. Hou, L. Gang, D. Jia, Solid State Sci., 42 (2015) 1726-1730.
[31] Z.P. Li, B.H. Liu, N. Morigasaki, S. Suda, J. Alloys Compd., 354 (2003) 243-247.
[32] Ç. Çakanyıldırım, M. Gürü, Renewable Energy, 35 (2010) 1895-1899.
[33] W. Chen, L.Z. Ouyang, J.W. Liu, X.D. Yao, H. Wang, Z.W. Liu, M. Zhu, J. Power Sources, 359 (2017) 400-407.
[34] A.K. Figen, S. Pişkin, Int. J. Hydrogen Energy, 38 (2013) 3702-3709.
[35] B.H. Liu, Z.P. Li, J.K. Zhu, J. Alloys Compd., 476 (2009) L16-L20.